

# New Organic Compounds Detection and Potential Removal in Crude Phosphoric Acid using Waste Sludge

**Saber Ahmed Ibrahim**

National Research Centre

**Ahmed Masoud**

NMA: Nuclear Materials Authority

**Mohamed Helmy Taha**

Nuclear Materials Authority

**Amr Sayed Meawad** (✉ [ameawad@science.helwan.edu.eg](mailto:ameawad@science.helwan.edu.eg))

Helwan University Faculty of Science <https://orcid.org/0000-0003-0061-6027>

---

## Research Article

**Keywords:** Waste sludge, Crude phosphoric acid, Organic species, Sorption

**Posted Date:** February 8th, 2021

**DOI:** <https://doi.org/10.21203/rs.3.rs-157157/v1>

**License:**  This work is licensed under a Creative Commons Attribution 4.0 International License.

[Read Full License](#)

---

1 **New Organic Compounds Detection and Potential Removal in Crude Phosphoric Acid using**  
2 **Waste Sludge**

3 Saber A. Ibrahim<sup>1</sup>, Ahmed M. Masoud<sup>2</sup>, Mohamed H. Taha<sup>2</sup>, Amr S. Meawad \*<sup>3</sup>

4 <sup>1</sup>Packaging Materials Department, National Research Centre, Elbehoth Street 33, 12622, Dokki, Cairo,  
5 Egypt.

6 <sup>2</sup>Nuclear Materials Authority, P.O. Box 530, El Maddi, Cairo, Egypt

7 <sup>3</sup>Chemistry Department, Faculty of Science, Helwan University, 11795, Cairo, Egypt,  
8  
9  
10  
11  
12  
13  
14  
15  
16  
17  
18  
19  
20  
21  
22  
23  
24

25 **Abstract**

26 Some organic compounds in phosphoric acid are a potential mediator of adverse environmental impacts  
27 on soil. This work aims to detect and reduce the content of organic compounds in crude phosphoric acid  
28 using waste sludge, from water treatment plants, as a low-cost sorbent. Gas chromatography/Mass  
29 spectrometry (GC/MS) was used to detect the organic species in crude phosphoric acid, while X-ray  
30 fluorescence (XRF), X-ray Diffraction (XRD), and Attenuated total reflectance Fourier transform  
31 infrared (ATR-FTIR) spectroscopy were used to characterize waste sludges. Practically, three sludge  
32 samples were utilized and different factors including shaking time, sorbent dose, and phosphoric acid  
33 concentration were studied.

34 The results of GC/MS revealed that crude phosphoric acid contains bis [tert-butyl(dimethyl)silyl]  
35 azelaate, dibutyl phthalate, and 2,6-di-tert-butyl-4-methylphenol as the main organic species. Moreover,  
36 the clay content and the surface charge of sludge strongly affect the removal efficiency of organic  
37 species. Kinetic analysis using Lagregran pseudo-first-order, pseudo-second-order, Morris-Weber, and  
38 Elvoich models display that the sorption process using waste sludges is a chemisorption process. Finally,  
39 the three sludge samples exhibit potential sorbents for the clarification of phosphoric acid and  
40 sequentially to produce green phosphate fertilizers.

41

42 **Keywords:**

43 Waste sludge; Crude phosphoric acid; Organic species; Sorption

44

45 **1. Introduction**

46 Phosphorus (P) is one of the vital macronutrients required for plant growth as well as human life.  
47 Phosphorus was utilized for increasing crop products since the 1950s (Stewart and Roberts 2012). The  
48 United Nations reported that the world population is expected to become about 9 billion by 2050, and  
49 the food demand will increase by 60% for the same period that subsequently will rise the global  
50 phosphorus demand (FAO 2018). Phosphorus security is considered one of the greatest global  
51 sustainability challenges in the twenty-first century (Cordell and White 2014). Phosphorus management  
52 is very important for sustainable food and agriculture, particularly in food-deficient and phosphorus-  
53 scarce countries (Cordell et al. 2015).

54 Phosphate rock is a nonrenewable natural resource that is used to describe phosphate-bearing minerals.  
55 Approximately 90% of the phosphate rock production worldwide is utilized in the fertilizer industry, and  
56 the other 10% is used in the animal feeds, detergents, and chemicals industries (Hellal et al. 2019;  
57 Nedelciu et al. 2020). Phosphate rock sources may be sedimentary origin as in Florida, Jordan, North  
58 Africa, and igneous origin as in South Africa, Brazil, Russia, or secondarily metamorphic origin as in  
59 India. Phosphate rocks exhibit different chemical, physical, and crystallographic characteristics based  
60 on its geological history and origin (Fayiga and Nwoke 2016).

61 It is well known that phosphate rocks contain organic compounds as a result of the biological  
62 sedimentation of sea organisms (Taha et al. 2019). In addition to organic compounds, phosphate rock is  
63 contains different hazardous elements such as U, Cd, and As (Fayiga and Nwoke 2016). Organic  
64 compounds as well as other harmful elements are introduced to phosphoric acid and phosphate fertilizers  
65 during the acidulation of phosphate rock (Zhang and Zhang 2010; Fayiga and Nwoke 2016). Most of  
66 previous studies reported that the organic compounds in the phosphoric acid mainly consists of humic  
67 compounds, aromatics, and other saturated and unsaturated fatty acids (Awwad et al. 2013; Hamza et al.

68 2013; Fawzy et al. 2018; El Naggar et al. 2019), however, , the main organic compounds in wet crude  
69 phosphoric acid have not been detected.

70 Organic compounds present in phosphoric acid have a negative impact on the quality and the quantity  
71 of the produced phosphoric acid whereas they give a dark color to the produced acid and affect the  
72 crystallization of the phosphogypsum (Singh et al. 2016; Taha et al. 2019). Furthermore, organic  
73 compounds result in serious operating problems during the application of liquid-liquid method for the  
74 recovery of uranium from phosphoric acid as well as the purification of phosphoric acid, whereas organic  
75 compounds accumulates and coagulates heavily at the interfacial area between the phosphoric acid and  
76 organic solvent which leads to the losses of the organic solvent and negatively impact on the process  
77 economy (Dissanayake and Chandrajith 2009; Awwad et al. 2013; Singh et al. 2016; El Naggar et al.  
78 2019). Also, organic compounds forms stable toxic complexes with the harmful elements in the  
79 phosphoric acid, which accumulate in the environment as a result of the continuous application of  
80 phosphate fertilizers and also transfer to the human body through the food chain (Fayiga and Nwoke  
81 2016; Taha et al. 2019).

82 Accordingly, the reduction of the organic compound from phosphoric acid is an important process in  
83 respect to improve the quality of phosphoric acid and produce eco-friendly fertilizers. Various methods  
84 were applied for the reduction of organic compounds from crude phosphoric acid for example liquid-  
85 liquid extraction or sorption (Awwad et al. 2013; Hamza et al. 2013; Singh et al. 2016; Fawzy et al.  
86 2018; El Naggar et al. 2019). Several materials were investigated for achieving this proposes such as  
87 clays (Hamza et al. 2015; Singh et al. 2016) and activated bio-chars (El Naggar et al. 2019; Taha et al.  
88 2019).

89 Sludge is the waste materials generated from water treatment plant. The production of sludge is expected  
90 to be increased shortly as a result of urbanization and industrial development (Rashed 2018). The  
91 chemical and physical properties of the sludge are varied as a result of the difference in the water

92 treatment technology, hydrogeology, and geology of the intake area, as well as the chemical composition  
93 of the utilized raw materials (Evuti and Lawal; Wołowiec and Bajda 2017). The management of sludge  
94 could be performed using several methods such as landfilling (Grassi et al. 2012), road surfacing  
95 (Jamshidi et al. 2012), and incineration (Yu and Zhong 2006).

96 Proper management of sludge in an eco-friendly and economical manner is very interesting. Sludge has  
97 good sorption properties (Yu and Zhong 2006). Recently, sludge has been utilized for the elimination of  
98 heavy metals from wastewater (Ragheb 2018; Rashed 2018; Wołowiec et al. 2019; Bogusz et al. 2019).  
99 However, sludge has never been applied for the purification of industrial phosphoric acid. In this regard,  
100 the present work aims to detect the main organic compounds in crude phosphoric acid as well as the  
101 application of waste sludge as an efficient sorbent for the retention of organic species through batch  
102 investigation in order produce eco-friendly phosphate fertilizers and reduce the accumulation of sludge  
103 in the environment.

## 104 **2. Experimental procedures**

### 105 **2.1. Materials**

106 Sludge samples designated here as S1, S2, and S3, were collected from three different water treatment  
107 stations namely El-Marg, Al-Obour, and El-Sheikh Zayed, respectively. The samples were washed with  
108 double distilled water, left overnight in an oven at 110 °C for complete drying, and finally left for cooling  
109 in a desiccator for further analysis.

110 Commercial crude phosphoric acid, containing ( $P_2O_5 = 26.5\%$ ,  $CaO = 0.34\%$ ,  $Fe_2O_3 = 1.1\%$ ,  $F = 0.64\%$ ,  
111  $U(VI) = 40$  ppm and organic compounds = 450 ppm) was purchased from Abu Zaabal Company for  
112 Fertilizer and Chemical Materials. Shimazu UV-visible 160 A spectrophotometer was used to determine  
113 the content of organic compounds, iron and uranium.

### 114 **2.2. Characterization methods**

115 X-ray Fluorescence (XRF) spectroscopy (Axios, sequential WD-XRF spectrometer, PANalytical) was  
116 used to determine the chemical composition of sludge samples. The phase composition of sludge samples  
117 was determined using X-ray diffraction (XRD, Bruker D8 advance X-ray diffractometer). The patterns  
118 were recorded by Cu-K $\alpha$  radiation with  $\lambda$  of 1.5406 Å and 40 kV tube voltage, 40 mA tube current, 2 $\theta$  scan  
119 range of 4–90°, 0.01° step width, and scan speed 0.5°/min. X'Pert High Score<sup>TM</sup> (version 2.0.1) was used  
120 to perform a semi-quantitative analysis of the crystalline phases in the sludge samples (Degen et al. 2014).  
121 Attenuated total reflectance Fourier transform infrared (ATR-FTIR) spectroscopy (Spectrum Two IR  
122 Spectrometer - PerkinElmer, Inc., Shelton, USA) was used to identify the main functional groups of sludge  
123 samples. acquisition conditions were 64 scans and 4 cm<sup>-1</sup> resolution in wavenumbers ranging from 4000  
124 to 400 cm<sup>-1</sup>.

125 The mean diameter of the sludge particles was determined at 170°, by dynamic light scattering (DLS)  
126 (NICOMP 380 ZLS, PSS, Santa Barbara, CA, USA). Also, the zeta potentials of the three samples were  
127 measured at 18°. Nitrogen adsorption-desorption measurements were carried out at 77.35 K on a Nova  
128 Touch LX<sup>4</sup> Quantachrome, USA to determine the Brunauer–Emmett–Teller (BET) surface area. Before  
129 measurement, samples were kept in a desiccator until testing. Samples were cooled with liquid nitrogen  
130 and analyzed by measuring the volume of gas (N<sub>2</sub>) adsorbed at specific pressures. The pore volume was  
131 taken from the adsorption branch of the isotherm at P/P<sub>0</sub> = 0.995 assuming complete pore saturation.

132 Gas chromatography/mass spectrometry (GC/MS) HP5890 Series II Gas Chromatograph, HP 5972 Mass  
133 Selective Detector and Agilent 6890 Series Autosampler (Agilent Technologies, USA) was used to  
134 identify the chemical constituents of crud phosphoric acid solution. A Supelco MDN-5S 30 m × 0.25 mm  
135 capillary column with a 0.5 µm film thickness was used with helium as the carrier gas at a flow rate of 1.0  
136 mL/min. The GC oven temperature was programmed at an initial temperature of 40 °C for 5 minutes, then  
137 heated up to 140 °C at 5 °C /min and held at 140 °C for 5 min, then heated to 280 °C at 9 °C/min and held  
138 for five additional minutes. Injector and detector temperatures were set at 250 °C. Mass spectrometry was

139 run in the electron impact mode (EI) at 70 eV. The identification of the chemical constituents was  
140 determined by their GC retention times, retention indices, and interpretation of their mass spectra and  
141 confirmed by mass spectral library search using the National Institute of Standards and Technology  
142 (NIST) database with those of authentic samples or published data (Shahat et al. 2011). The retention  
143 indices were calculated for all of the volatile constituents using a homologous series of C8-C20 n-alkanes.

### 144 **2.3. Sorption methodology**

145 The three sludge samples were investigated for the sorption of organic species from crude phosphoric  
146 acid (4.5 M) in batch technique. All tests were achieved in polyethylene type using a thermostatic shaking  
147 water bath. The influence of reaction time, sludge amount of addition, phosphoric acid concentration on  
148 the removal percent have been examined. In details, 40 mL of liquid phase has been shaken with 0.4 g  
149 of the sorbent at  $298 \pm 1$  K for 24 hrs. The mean values  $\leq 4\%$  relative errors were accepted for the  
150 performed experiments. After equilibration, the sludge was removed from the phosphoric acid. The  
151 concentration of organic compounds in crude acid has been measured using a spectrophotometer at 418  
152 nm (Taha et al. 2019).

153 The following equations have been applied to figure out the impact of the main variables on the removal  
154 efficiency of organic compounds from industrial phosphoric acid:

$$155 \quad E \% = \frac{1 - C_e}{C_o} \times 100\% \dots \dots (1)$$

$$156 \quad q_e = C_o - C_e \times \frac{V}{m} \dots \dots (2)$$

157 where  $C_o$  and  $C_e$  are the OM concentration ( $\text{mg L}^{-1}$ ) before the adsorption and at equilibrium,  
158 respectively,  $q_e$  ( $\text{mg g}^{-1}$ ) is the amount of OM sorbet,  $V$  is the volume of phosphoric acid (L), and  $m$  is  
159 the mass of the sludge (g).

## 160 **3. Results and Discussions**

### 161 **3.1. Characterization of sludge samples**

162 **3.1.1. Physical characterization**

163 Particle size distributions of different sludge samples were investigated to examine the mean particle  
164 size and polydispersity index of Gaussian distribution. The samples S1, S2 and S3 were measured and  
165 the bell shape distribution forms were clearly detectable in **Fig. 1a**. The mean particle sizes for S1, S2  
166 and S3 are 1725, 748 and 755 nm, respectively. In addition, the poly dispersity index was laid between  
167 0.2 and 0.5 that indicated to unimodal particle size with narrow distributions (Ibrahim and Voit 2009).  
168 Selected sludges were directly measured without further treatment like grinding or burning. Big clusters  
169 of sludge with accumulated inorganic and organic substance resulted from Nile River were presence in  
170 range 0.7 to 1.7  $\mu\text{m}$ . neither big particles of sludge nor excellent polydispersity indices were pointed to  
171 homogenized particle size (Ahmed et al. 2019; Meawad and Ibrahim 2019).

172 Zeta potential has a great affect in the stability of dispersed solution from sludge in aqueous medium.  
173 The average zeta potentials of sludge over 11 measurements for each sample were illustrated in **Fig. 1b**.  
174 Investigated sludge samples S1, S2 and S3 by DLS measurements with mean zeta potential -5.55, -27.93  
175 and -34.14 mV, respectively. In addition, the average mobilities of dispersed particles were -0.39, -2.02  
176 and -2.38 M.U. for S1, S2 and S3, respectively. Previous results indicated to the stability of samples S2  
177 and S3 are higher than S1 with low mobility and low zeta potential. The separation of organic  
178 compounds was depending on the fast precipitation of sludge during physical adsorption mechanism.

179 The surface area is one of unique phenomena related to the particle size with inverse proportions  
180 (Ibrahim et al. 2018). Surface area measurement with related indices for sludge samples were tabulated  
181 in Table 1. The isotherm branch of nitrogen gas on dry degassed sludge power with adsorption trend  
182 were applied to calculate BET values 19, 94 and 102  $\text{m}^2/\text{g}$  for sludge sample S1, S2 and S3, respectively.  
183 The adsorption indices were indicated to perfect trend of measured points with correlation coefficient  
184  $\approx 1$  as first order equation of linear relationship. The particle size results have a great agreement with  
185 confirmation to each other's through increasing the surface area with decreasing of particle size from

186 S3, S2 to S1. Overall, the physical characterization measurements are verified the stability, size and  
187 surface area for sludge samples as mentioned theoretically and previous research (Ibrahim et al. 2016;  
188 Meawad and Ibrahim 2019; Abdelraof et al. 2020).

### 189 **3.1.2. Chemical characterization**

190 The chemical composition of sludge samples is presented in Table 2. The XRF analysis shows that silica  
191 and alumina are the main oxides of the three sludges due to the precipitated clay. **Fig. 2** shows the FTIR  
192 spectra of the three sludge samples. In all spectra, the bands at  $3400\text{ cm}^{-1}$  and  $1630\text{ cm}^{-1}$  are related to  
193 the stretching and bending vibrations of -OH group of the interlayer water molecule, respectively. The  
194 band located at  $1070\text{ cm}^{-1}$  assigned to T-O-Si (T = Si or Al) asymmetric stretching. Other significant  
195 bands are related to symmetric stretching of Si-O-Si and bending of Si-O are located at around  $800\text{ cm}^{-1}$   
196 and  $455\text{ cm}^{-1}$ , respectively. The presence of such bands confirms the mineralogical analysis about the  
197 presence of aluminosilicate phases in sludge samples. Furthermore, the peak around  $1400\text{ cm}^{-1}$  is likely  
198 attributed to carbonate species, while the peaks at  $2900\text{ cm}^{-1}$  and  $2985\text{ cm}^{-1}$  correspond to stretches of  
199 C-H carbons of organic species in S2 sludge. The results of XRD, **Fig. 3**, indicated the presence of  
200 feldspar-type minerals, quartz, clay minerals (illite, kaolinite and chlorite), carbonate minerals (calcite,  
201 aragonite and dolomite) as main crystalline phases as well as mica, anhydrite, apatite and other minerals  
202 as minor phases. The related semi-quantitative data are presented in Table 3. It is well known that the  
203 clay minerals content and the charge on clay surface play an important role in the efficient sorption of  
204 organic compounds (Lützow et al. 2006; Setia et al. 2014). As shown, the total clay content in S1 is  
205 higher than that in S2 and S3, while the feldspar content is much lower. Moreover, the quartz content in  
206 S1 and S2 are much higher than that in S3.

### 207 **3.2. Detection of organic constituent in crude phosphoric acid**

208 The accumulation of organic compound as well as potentially toxic elements in the environment has  
209 becomes a global concern. Continuous application of phosphate fertilizers will increase the accumulation

210 of the organic compounds and other hazardous to the ecosystems. Therefore, the detection of the main  
211 organic compounds in crude phosphoric acid is important for a successive process for the removal of  
212 these contaminants.

213 The obtained results in **Fig.4** clear that the main organic compounds in crude phosphoric acid is mainly  
214 composed of three components: azelaic acid (diTBDMS: (Bis [tert-butyl(dimethyl)silyl] azelaate),  
215 Butylated hydroxytoluene (2,6-Di-tert-butyl-4-methylphenol), and Dibutyl phthalate.

216 Azelaic acid, diTBDMS is a saturated dicarboxylic acid that belongs to the class of organic compounds  
217 known as medium-chain fatty acids. It has the following formula and molecular weight:  $C_{21}H_{44}O_4Si_2$   
218 and 416.74 g/mol (Wheeler et al. 2000). 2, 6-Di-tert-butyl-4-methylphenol (Butylated hydroxytoluene)  
219 is a lipophilic organic compound with a chemical formula of  $C_{15}H_{24}O$  and a molecular mass of 220.35  
220 g/mol (US National Library of Medicine 2020). Butylated hydroxytoluene (BHT) is a member of the  
221 alkyl phenols broad group which has been widely used as an antioxidant food additive. BHT is rapidly  
222 decomposed forming different metabolites in the environment such as in water and soils (Ryssel et al.  
223 2015). BHT is hardly biodegradable and therefore the bioaccumulation of BHT and its derivatives  
224 exhibit high toxicity to aquatic organisms, and they are considered as a human health risk from a food  
225 safety point of view. The BHT and its metabolites are on the undesirable substances list "Danish  
226 Environmental Protection Agency" (Norwegian Scientific Committee for Food Safety 2009; Ryssel et  
227 al. 2015).

228 Dibutyl phthalate (DBP) it is a phthalate ester with the following formula and molecular mass:  $C_{16}H_{22}O_4$   
229 and 278.34 g/mol (2020). Dibutyl phthalate is a ubiquitous environmental contaminant that is used  
230 widely as plasticizer in modern agricultural production due to wastewater irrigation, and the common  
231 applications of agricultural chemicals (He et al. 2015). The U.S. Environmental Protection Agency  
232 classified the Dibutyl phthalate as an endocrine disruptor chemical and an environmental pollutant,

233 which means that the distribution of DBP through the soil poses threats to both the environment as  
234 well as the human food chain (Bui et al. 2016).

### 235 **3.3. Sorption investigation**

236 The following section discusses the application of three sludge wastes for the clarification of crude  
237 phosphoric acid in order to obtain a proper acid for clean fertilizers. The impact of shaking time,  
238 phosphoric acid concentration, and sludge amount of addition, as main variables, on the organic  
239 compounds adsorption percent have been tested. The sorption isotherms, as well as kinetics, have been  
240 performed in order to provide useful data required for the scale-up experiments and the process design.

#### 241 **3.3.1. Effect of shaking time**

242 Several experiments were achieved to investigate the impact of reaction time in the range of 1-120 min  
243 on organic species sorption from commercial phosphoric acid (4.5 M) using different sludge wastes. In  
244 detail, the three waste sludge has been shaken with crude phosphoric acid with sorbent dose of 10.0 g/  
245 L, shaking speed of 150 rpm, and room temperature.

246 The variation of organic compounds adsorption percent as a function of shaking time has been illustrated  
247 in **Fig.5**. From the data, it is evident that the sorption of organic species from industrial phosphoric acid  
248 by the three sludge is a fast reaction whereas the reaction equilibrium is obtained after 30 min for the  
249 three sorbents. In addition, the three sorbent exhibit the same sorption performance whereas the sorption  
250 reaction consists of two stages; the first stage starts from 1 to 30 min and is characterized by a high  
251 adsorption rate of reaction. Numerically, organic compounds sorption efficiency increased from 19.0 to  
252 54.0 for S1, from 13.1 to 48.0 for S2, and 17.8 to 48.4% for S3, as the shaking time increased from 1 to  
253 30 min respectively. This behavior may be due to the presence of free active sites on the surface of the  
254 waste sludge (Zhang et al. 2015; Taha et al. 2018). The second stage shows a slow rate of reaction  
255 whereas the organic compounds sorption percent is slightly varied from about 54.0 to 58.5% for S1,  
256 from 48.0 to 51.7% for S2, and from 48.4 to 50.7% for S3 as the shaking time increase from 30 to 120

257 min. This performance may be due to that most of the sorbent surface active sites were occupied,  
258 therefore organic compounds molecules need more time for the diffusion and reaction with the inside  
259 active groups (Zhang et al. 2015; Taha et al. 2018). This was consistent with other previous reports  
260 (Nawar et al. 2015; Ait Ahsaine et al. 2017; Ali et al. 2019; Taha et al. 2019). To ensure that complete  
261 equilibrium was attained, other subsequent experiments were performed at 120 min.

### 262 **3.3.2. Influence of phosphoric acid concentration**

263 To investigate the impact of phosphoric acid concentrations ranging from 4.5 to 8.0 M on the sorption  
264 of organic compounds using different waste sludge sorbents, a set of experiments were achieved at 120  
265 min reaction time, 100 rpm stirring speed, and  $25 \pm 1$  °C. The collected data has been illustrated in **Fig.**  
266 **6** as a relation between organic compounds sorption % and phosphoric acid molarity. The exhibited data  
267 declare that the increase in phosphoric acid concentration has the same impact on the sorption behavior  
268 of the three investigated waste sludge sorbents. In details, organic compounds sorption efficiency has  
269 drastically reduced from 59.0 to 30.2% for S1, from 52.3 to 26.0% for S2, and from 50.7 to 22.9% for  
270 S3 sorbent as the phosphoric acid concentration increased from 4.5 to 8.0 M. This behavior could be  
271 attributed to that as the phosphoric acid molarity increases, the number of phosphoric acid molecules  
272 increases which, in turn, increase the coverage of the surface active sites of the sorbent particles by the  
273 excess acid molecules and in turn decrease the sorption capability of the sorbent. Also, the increase of  
274 acid molarity results in the increase of the acid bulk density which effects negatively on the diffusion of  
275 the organic compounds molecules to the sorbent surface (Morsy and Hussein 2012; Taha et al. 2019).

### 276 **3.3.3. Effect of sorbent dose**

277 **Fig.7** explores the impact of S1, S2, and S3 waste sludge amount of addition on the reduction of organic  
278 compounds from industrial phosphoric acid. In details, the sorbent amount of addition covers the range  
279 from 0.5 to 20 g/L however, the other controlling conditions were kept at a phosphoric acid concentration  
280 of 4.5 M, room temperature, 100 rpm stirring speed, and 120 min shaking time, to optimize the required

281 sorbet dose for maximum organic compounds removal. It is obvious that the organic compounds  
282 adsorption percent increases by increasing the three waste sludge sorbents' amount of addition. This  
283 performance may be attributed to the existence of more active reaction sites as the sorbent dose increases  
284 (Zou et al. 2017; El Naggar et al. 2019). Numerically, The organic compounds sorption changed from  
285 16.2 to 71.5% for S1, from 11.0 to 61.7% for S2, and from 13.5 to 59.1% for S3 sorbent as the waste  
286 sludge dose increased from 0.5 to 20.0g L<sup>-1</sup>. It is worth noted that, the sorption capacity of the  
287 investigated three waste sludge sorbents negatively impacted by the increase in the sorbent amount of  
288 addition. Specifically, the sorption capacity, q<sub>e</sub> value, decreased from 145.6 to 16.1 mg/ g for S1, from  
289 99.0 to 13.9 mg g<sup>-1</sup> for S2, and from 121.5 to 13.3 mg g<sup>-1</sup> for S3 as the sorbent dose increased from 0.5  
290 to 20.0 g L<sup>-1</sup>. This performance could be attributed to the sorbent active sites were not freely available for  
291 binding with organic compounds molecules, and the low concentration of organic compounds species  
292 could not meet the adsorption capacities of adsorbents, and thereby decreased the q<sub>e</sub> (Zou et al. 2017; El  
293 Naggar et al. 2019). This result is consistent with studies applying alum sludge and sewage sludge for  
294 wastewater treatment (Nawar et al. 2015; Abo-El-Enein et al. 2017).

### 295 **3.4. The uptake kinetics**

296 The uptake kinetics is important in the solid-liquid reactions for better understanding the rate of reaction  
297 and the possible adsorption mechanism. In this section, the kinetics of OM removal from industrial  
298 phosphoric acid using S1, S2, and S3 waste sludge were performed. Accordingly; the equations of the  
299 following kinetic models namely; pseudo-first-order, pseudo-second-order, Elvoich, and Weber and  
300 Morris kinetic models (Eq. (3), Eq. (4), Eq. (5) and Eq. (6) respectively) have been applied to the  
301 adsorption data as shown in **Figs. 8-11**, respectively (Kim and Kim 2019; Kang and Kim 2019). The  
302 values of the kinetic model constants have been calculated and displayed in Table 4. The coefficient of  
303 correlation (R<sup>2</sup>), was employed to figure out the best kinetic equation for describing the resin- metal ions  
304 interaction.

305 
$$\text{Log} (q_e - q_t) = \text{Log} q_e - \left(\frac{K_1}{2.303}\right) t \dots \dots (3)$$

306 
$$\frac{t}{q_t} = \frac{1}{K_2 q_e^2} + \left(\frac{1}{q_e}\right) t \dots \dots (4)$$

307 
$$q_t = \frac{1}{\beta} \ln(\alpha\beta) + \frac{1}{\beta} \ln t \dots \dots (5)$$

308 
$$q_t = K_{id} t^{0.5} + C \dots \dots (6)$$

309 Where  $q_t$  is the sorption capacity at time  $t$  ( $\text{mg g}^{-1}$ );  $K_1$  is the rate constant of the pseudo first-order  
 310 sorption ( $\text{min}^{-1}$ ),  $t$  is time (min);  $K_2$  is the rate constant of the pseudo second order kinetics ( $\text{g/mg min}$ );  
 311  $\beta$  is referred to the surface coverage extension and the activated energy for chemisorption and  $\alpha$  ( $\text{mg/g}$   
 312 min) is the initial adsorption rate;  $K_{id}$  is intraparticle diffusion rate constant ( $\text{mg/g. min}^{1/2}$ );  $C$  is the  
 313 initial adsorption ( $\text{mg g}^{-1}$ ).

314 The experimental data have been analyzed using the Pseudo-first order equation as explored in **Fig. 8**.  
 315 The Figure obvious that the relation between Log ( $q_e - q_t$ ) vs time yield straight lines with poor correlation  
 316 coefficient which indicated that the organic compounds sorption process is not fitted well with the  
 317 Lagergren equation. In many cases in the literature, Lagergren kinetic model was commonly is not fitting  
 318 well for the whole reaction times, however it applicable only for describing initial stage of the sorption  
 319 processes (Ait Ahsaine et al. 2017). The Pseudo-second order reaction equation (McKay equation) was  
 320 examined to fit the obtained results as shown in **Fig. 9**. It is obvious that the relation between  $t/q_t$  as a  
 321 function of sorption time gives an excellent linear relationship with a correlation coefficient equal to  
 322 0.99 for the investigated three waste sludge. Besides, the experimental sorption capacity  $q_{e \text{ exp}}$  for S1,  
 323 S2, and S3 sorbents is consistent with the calculated sorption capacity  $q_{e \text{ cal}}$ . This evidence that the  
 324 Pseudo-second order kinetic equation could be successfully describe the organic compounds sorption  
 325 from crude phosphoric acid using S1, S2, and S3 sludge. This means that the organic compounds sorption  
 326 process is chemisorption and there is electron transfer or electron sharing between the applied waste

327 sludge sorbents and the organic compounds species (Taha et al. 2018, 2019). This results in consistent  
328 with other previous reports (Hamza et al. 2013; Ait Ahsaine et al. 2017; Ali et al. 2019; Taha et al. 2019).  
329 The half-equilibrium time,  $t_{1/2}$  (h), and the initial adsorption rate,  $h$  (mol/ g. h) for S1, S2 and S3 waste  
330 sludge sorbents were calculated from equations 1 and equation presented in (El Naggar et al. 2019). The  
331 explored results in Table 4 reveal that S2 sludge has the highest half-equilibrium time (5.3) while S3 has  
332 the lowest value (3.6). Nevertheless, S1 and S3 sorbents have the greatest initial adsorption rate (6.69  
333 and 6.55 mol/g.h) and S2 sorbent has the lowest value (4.6 mol/g.h). The sorption capacity at equilibrium  
334 for the three applied sludge sorbents could rank as the following  $S1 > S2 > S3$ . It worth noted that the  
335 S3 sorbent has the highest surface area ( $m^2/g$ ) followed by S2 ( $m^2/g$ ) and then S1 sorbent ( $m^2/g$ ) even  
336 though, S3 sorbent exhibits the lowest sorption capacity and S1 show the highest organic compounds  
337 sorption capacity. This means that the synergistic effect of the sorbent surface area is not the only  
338 parameter that controls the sorption process however there are other parameters that may be exhibit anti-  
339 synergistic effects such as the net charge of the sorbent surface. From the zeta potential analysis for the  
340 applied three sorbents, it is clear that S2 and S3 have a highly negative surface (-27.9 and -34.2 mV  
341 respectively) which in turn results in the repulsion between the sorbent particles and the formation of  
342 unstable complexes with the organic compounds species. However, S1 has a much lower surface charge  
343 (-5.6 mV) which means that it could produce more stable complexes with organic compounds.

344 The mathematical treatment of the obtained results using Elovich equation has been performed to figure  
345 out where the organic compounds adsorption process is chemical adsorption in nature or not. The plot  
346 of  $\ln t$  versus  $qt$ , **Fig. 10**, explore straight lines with a good correlation coefficient (about 0.95) for S1,  
347 S2, and S3 waste sludge sorbent. This confirms that the organic compounds adsorption from crude  
348 phosphoric acid using S1, S2, and S3 is a chemisorption process and the adsorption rate is exponentially  
349 dependent on the number of available adsorption sites in the applied sorbents (Ali et al. 2019). Table  
350 4 declares that the initial adsorption rate for S1, S2, and S3 sorbents are 31.6, 14.9, and 32.8 mg/g.min

351 respectively. It is worth noted that, the initial sorption rate value ( $\alpha$ ) obtained from Elvoich model has  
352 the same trend as the initial sorption rate ( $h$ ) obtained from McKay equation whereas  $S1 \approx S3 > S2$ .  
353 Nevertheless,  $\alpha$  values are 4-5 times greater than  $h$  values.

354 Despite Pseudo-second order and Elovich kinetic models have been successfully described the nature of  
355 the organic compounds sorption process as a chemisorption reaction however, they could not give clear  
356 information regards to the organic compounds adsorption mechanism. In the solid-liquid reactions, the  
357 sorption kinetics could be controlled with numerous diffusion mechanisms; resistance to bulk diffusion,  
358 film diffusion, and intraparticle diffusion. Mainly, the resistance to film diffusion is active at the  
359 beginning of the sludge sorbents and liquid phosphoric acid. Also, by applying sufficient velocity for  
360 mixing the sludge sorbents and phosphoric acid, the effect of the resistance to bulk diffusion could be  
361 overlooked. Thus, the resistance to intraparticle diffusion is the main controlling step. Accordingly, the  
362 obtained experimental results have been analyzed using the Morris-Weber model as shown in **Fig. 11**.  
363 The model constants were evaluated from the plot of  $qt$  as a function of  $t^{0.5}$  and presented in Table 4.  
364 **Fig. 11** displays two regions (multi-linear relationship) for S1, S2, and S3 sorbents which means that the  
365 intraparticle diffusion is not the only mechanism that controls the organic compounds sorption proces.  
366 This may be due to the rate of transfer of the organic compounds molecules is not the same in both  
367 sorption stages; initial and final which clears the effect of the boundary layer (Wu et al. 2009). Table 4  
368 evident that the first stage of the organic compounds adsorption process is characterized by low boundary  
369 layer effect and in turn high sorption rate for the applied three sorbents which confirm the fast reaction.  
370 The reason beyond that may be the presence of avialable surface active sites which result in the external  
371 surface adsorption (Wu et al. 2009; Taha et al. 2019). On the contrary, the second stage is characterized  
372 by a low absorption rate and high boundary layer effect for S1, S2, and S3 sludge which could be  
373 attributed to the saturation of most sludge surface sites, accordingly the intraparticle diffusion (IPD)  
374 begins. In this regard, it could be indicated that the sorption of organic species from commercial

375 phosphoric acid using S1, S2, and S3 sewage sludge is controlled by the combination of external surface  
376 adsorption and intraparticle diffusion as rate-controlling steps (Ait Ahsaine et al. 2017; Taha et al. 2019).  
377 The adsorption capacity of S1, S2 and S3 sludge sorbents has been compared with other adsorbents that  
378 applied for the same purpose, removal of organic compounds recovery from crude phosphoric acid, and  
379 exhibited in Table 5. The revealed data declare that the utilized three sorbents; S1, S2 and S3 possess  
380 organic compounds sorption capacity within the given sorbents from literature which obvious that these  
381 swage sludges could be applied for the clarification of crude phosphoric acid.

### 382 **3.5. The sorption isotherm**

383 The sorption isotherm is an essential factor for the plant design and improving the adsorption system.  
384 Accordingly, Freundlich and Langmuir isotherm models were applied for analyzing the obtained  
385 equilibrium results. The coefficient of correlation ( $R^2$ ) has been applied for testing the fitting of the  
386 obtained data to the isotherm equations. The linear form of Freundlich and Langmuir isotherm models  
387 have commonly expressed equations 1 and 2, respectively (Hussein and Taha 2013):

$$388 \quad \log q_e = \log K_F + \frac{1}{n} \log C_e \dots \dots (7)$$

$$389 \quad \frac{C_e}{q_e} = \frac{1}{k_L q_m} + \frac{C_e}{q_m} \dots \dots (8)$$

390 where  $K_f$  (L/ mg) is corresponding to the sorption capacity, and  $n$  refers to the sorption intensity.  $q_m$  (mg.  
391  $g^{-1}$ ) is the maximum sorption capacity of the sorbent, and  $k_L$  (L.  $mg^{-1}$ ) is the equilibrium constant which,  
392 refers to the energy of adsorption and reflects the affinity of resin towards the organic compounds.

393 The isotherm parameters of Freundlich model have been evaluated from the illustration of  $\ln q_e$  as a  
394 function of  $\ln C_e$ , **Fig. 12**, and presented in Table 6. Nevertheless, the parameters of Langmuir model  
395 were obtained from the Figure of  $C_e/q_e$  as a function of  $C_e$  and displayed in Table 6.

396 The explored results in **Figs. 12 and 13** as well as Table 6, declare that only Freundlich isotherm plot  
397 gives a straight line with a perfect correlation coefficient (about 0.98) for all investigated sorbents. This

398 indicates that the organic compounds adsorption from crude dihydrate phosphoric acid using S1, S2, and  
399 S3 waste sludge is fitting Freundlich isotherm model which means a heterogeneous sorption system with  
400 different active sites. Furthermore, Table 6 shows that  $n > 1$  for the applied three waste sludge sorbents  
401 which obvious that the sorption is a physical process (Dacrory et al. 2020; Masoud 2020).

#### 402 **4. Conclusions**

403 Bis [tert-butyl(dimethyl)silyl] azelaate, 2,6-Di-tert-butyl-4-methylphenol, and Dibutyl phthalate  
404 compounds have been detected as the main organic compounds in crude phosphoric acid. Waste sludge  
405 namely, S1, S2 and S3, has been successfully utilized for the clarification of crude phosphoric acid. The  
406 main variables that affect the organic compounds sorption efficiency such as: shaking time, sorbent dose,  
407 and phosphoric acid concentration were studied. The revealed data declare that the adsorption reaction  
408 is fast whereas the reaction equilibrium has been reached after 30 min for the three investigated sorbents.  
409 The sorbent does have positive impact on the sorption percent on the other hand the phosphoric acid  
410 concentration has negative influence. The sorption kinetics has been performed using pseudo-first-order,  
411 pseudo-second order, Elvoich, and Weber-Morris kinetic models. The displayed results explore that the  
412 S1, S2 and S3 sorbent exhibit chemisorption reaction. S1 waste sludge exhibit the highest sorption  
413 capacity, while S3 shows the lowest sorption capacity.

414

415

416

417

418

419

420

421

422 **5. Declarations**

423 **5.1. Ethics approval and consent to participate**

424 Not applicable

425 **5.2. Consent for publication**

426 Not applicable

427 **5.3. Availability of data and materials**

428 All data generated or analysed during this study are included in this published article.

429 **5.4. Competing interests**

430 The authors declare that they have no competing interests.

431 **5.5. Funding**

432 The authors did not receive support from any organization for the submitted work.

433 The authors have no relevant financial or non-financial interests to disclose.

434 **5.6. Authors' contributions**

435 All authors have equal contributions in the established of the research ides, experimental part,  
436 characterization, and explanation of results and shared in writing and revise the manuscript.

437

438

439

440

441

442

443

444

445

446 **6. References**

- 447 Abdelraof M, Ibrahim S, Selim MH, Hasanin M (2020) Immobilization of L-methionine  $\gamma$ -lyase on  
448 different cellulosic materials and its potential application in green-selective synthesis of volatile  
449 sulfur compounds. *J Environ Chem Eng* 8:. <https://doi.org/10.1016/j.jece.2020.103870>
- 450 Abo-El-Enein SA, Shebl A, Abo El-Dahab SA (2017) Drinking water treatment sludge as an efficient  
451 adsorbent for heavy metals removal. *Appl Clay Sci* 146:343–349.  
452 <https://doi.org/10.1016/j.clay.2017.06.027>
- 453 Ahmed HM, Abdellatif MM, Ibrahim S, Abdellatif FHH (2019) Mini-emulsified Copolymer/Silica  
454 nanocomposite as effective binder and self-cleaning for textiles coating. *Prog Org Coatings* 129:52–  
455 58. <https://doi.org/10.1016/j.porgcoat.2019.01.002>
- 456 Ait Ahsaine H, Zbair M, El Haouti R (2017) Mesoporous treated sewage sludge as outstanding low-cost  
457 adsorbent for cadmium removal. *Desalin Water Treat* 85:330–338.  
458 <https://doi.org/10.5004/dwt.2017.21310>
- 459 Ali MM, Attia AA, Taha MH, et al (2019) Application of acid activated bentonite for efficient removal  
460 of organic pollutants from industrial phosphoric acid: Kinetic and thermodynamic study. In: *SPE*  
461 *Middle East Oil and Gas Show and Conference, MEOS, Proceedings*
- 462 Awwad NS, El-Nadi YA, Hamed MM (2013) Successive processes for purification and extraction of  
463 phosphoric acid produced by wet process. *Chem Eng Process - Process Intensif* 74:69–74.  
464 <https://doi.org/10.1016/j.cep.2012.11.009>
- 465 Bogusz A, Oleszczuk P, Dobrowolski R (2019) Adsorption and desorption of heavy metals by the  
466 sewage sludge and biochar-amended soil. *Environ Geochem Health* 41:1663–1674.  
467 <https://doi.org/10.1007/s10653-017-0036-1>
- 468 Bui TT, Giovanoulis G, Cousins AP, et al (2016) Human exposure, hazard and risk of alternative  
469 plasticizers to phthalate esters. *Sci. Total Environ.* 541:451–467

470 Cordell D, Turner A, Chong J (2015) The hidden cost of phosphate fertilizers: mapping multi-  
471 stakeholder supply chain risks and impacts from mine to fork. *Glob Chang Peace Secur* 27:323–343.  
472 <https://doi.org/10.1080/14781158.2015.1083540>

473 Cordell D, White S (2014) Life's bottleneck: Sustaining the world's phosphorus for a food secure future.  
474 *Annu. Rev. Environ. Resour.* 39:161–188

475 Dacrory S, Haggag ESA, Masoud AM, et al (2020) Innovative synthesis of modified cellulose derivative  
476 as a uranium adsorbent from carbonate solutions of radioactive deposits. *Cellulose* 27:7093–7108.  
477 <https://doi.org/10.1007/s10570-020-03272-w>

478 Degen T, Sadki M, Bron E, et al (2014) The high score suite. In: *Powder Diffraction*. pp S13–S18

479 Dissanayake CB, Chandrajith R (2009) Phosphate Mineral Fertilizers, trace metals and human health. *J.*  
480 *Natl. Sci. Found. Sri Lanka* 37:153–165

481 El Naggat AMA, Ali MM, Abdel Maksoud SA, et al (2019) Waste generated bio-char supported co-  
482 nanoparticles of nickel and cobalt oxides for efficient adsorption of uranium and organic pollutants  
483 from industrial phosphoric acid. *J Radioanal Nucl Chem* 320:741–755.  
484 <https://doi.org/10.1007/s10967-019-06529-2>

485 Evuti AM, Lawal M Recovery of coagulants from water works sludge: A review. [researchgate.net](https://www.researchgate.net)

486 FAO (2018) Feeding nine billion in 2050. In: Rome.  
487 <http://www.fao.org/news/story/en/item/174172/icode/>. Accessed 17 Nov 2020

488 Fawzy MM, Farag NM, Amin AS (2018) Treatment of Crude Phosphoric Acid from Some Undesirable  
489 Impurities. *J Basic Environ Sci* 5:204–216

490 Fayiga AO, Nwoke OC (2016) Phosphate rock: Origin, importance, environmental impacts, and future  
491 roles. *Environ. Rev.* 24:403–415

492 Grassi M, Kaykioglu G, Belgiorno V, Lofrano G (2012) Removal of Emerging Contaminants from  
493 Water and Wastewater by Adsorption Process. pp 15–37

- 494 Hamza W, Chtara C, Benzina M (2013) Retention of organic matter contained in industrial phosphoric  
495 acid solution by raw Tunisian clays: Kinetic equilibrium study. *J Chem* 2013:.  
496 <https://doi.org/10.1155/2013/218786>
- 497 Hamza W, Chtara C, Benzina M (2015) Characterization and application of Fe and iso-Ti-pillared  
498 bentonite on retention of organic matter contained in wet industrial phosphoric acid (54 %): kinetic  
499 study. *Res Chem Intermed* 41:6117–6140. <https://doi.org/10.1007/s11164-014-1726-2>
- 500 He L, Gielen G, Bolan NS, et al (2015) Contamination and remediation of phthalic acid esters in  
501 agricultural soils in China: a review. *Agron. Sustain. Dev.* 35:519–534
- 502 Hellal F, El-Sayed S, Zewainy R, Amer A (2019) Importance of phosphate rock application for  
503 sustaining agricultural production in Egypt. *Bull Natl Res Cent* 43:.  
504 <https://doi.org/10.1186/s42269-019-0050-9>
- 505 Hussein AEM, Taha MH (2013) Uranium removal from nitric acid raffinate solution by solvent  
506 immobilized PVC cement. *J Radioanal Nucl Chem* 295:709–715. <https://doi.org/10.1007/s10967-012-2158-3>
- 508 Ibrahim S, Abdel Rehim M, Turkey G (2018) Dielectric study of polystyrene/polycaprolactone  
509 composites prepared by miniemulsion polymerization. *J Phys Chem Solids* 119:56–61.  
510 <https://doi.org/10.1016/j.jpcs.2018.03.030>
- 511 Ibrahim S, Abdelfattah I, Soliman O (2016) Environmental recycling of compact disc using industrial  
512 wastewater. *Der Pharm Lett* 8:207–214
- 513 Ibrahim S, Voit B (2009) Synthesis and characterization of well-defined block copolymers by combing  
514 controlled radical and cationic polymerization. In: *Macromolecular Symposia*. pp 59–66
- 515 Jamshidi M, Jamshidi A, Mehrdadi N (2012) APPLICATION OF SEWAGE DRY SLUDGE IN  
516 CONCRETE MIXTURES
- 517 Kang HJ, Kim JH (2019) Adsorption Kinetics, Mechanism, Isotherm, and Thermodynamic Analysis of

518 Paclitaxel from Extracts of *Taxus chinensis* Cell Cultures onto Sylopute. *Biotechnol Bioprocess Eng*  
519 24:513–521. <https://doi.org/10.1007/s12257-019-0001-1>

520 Kim YS, Kim JH (2019) Isotherm, kinetic and thermodynamic studies on the adsorption of paclitaxel  
521 onto Sylopute. *J Chem Thermodyn* 130:104–113. <https://doi.org/10.1016/j.jct.2018.10.005>

522 Lützow M V., Kögel-Knabner I, Ekschmitt K, et al (2006) Stabilization of organic matter in temperate  
523 soils: Mechanisms and their relevance under different soil conditions - A review. *Eur. J. Soil Sci.*  
524 57:426–445

525 Masoud AM (2020) Sorption behavior of uranium from Sulfate media using purolite A400 as a strong  
526 base anion Exchange resin. *Int J Environ Anal Chem.*  
527 <https://doi.org/10.1080/03067319.2020.1763974>

528 Meawad A, Ibrahim S (2019) Novel bifunctional dispersing agents from waste PET packaging materials  
529 and interaction with cement. *Waste Manag* 85:563–573.  
530 <https://doi.org/10.1016/j.wasman.2019.01.028>

531 Morsy AMA, Hussein AEM (2012) Retention of Uranium from Liquid Waste Solution onto. *Arab Conf*  
532 *Peac use At Energy*

533 Nawar N, Ahmad ME, Said WM El, et al (2015) Adsorptive Removal of Phosphorous from Wastewater  
534 Using Drinking Water Treatment Alum Sludge (DWTAS) as Low Cost Adsorbent Citation. *Am J*  
535 *Chem Appl* 2:7985

536 Nedelciu CE, Ragnarsdóttir KV, Stjernquist I, Schellens MK (2020) Opening access to the black box:  
537 The need for reporting on the global phosphorus supply chain. *Ambio* 49:881–891.  
538 <https://doi.org/10.1007/s13280-019-01240-8>

539 Norwegian Scientific Committee for Food Safety (2009) Opinion of the Panel on Food Additives,  
540 Flavourings, Processing Aids, Materials in Contact with Food and Cosmetics of the Norwegian  
541 Scientific Committee for Food Safety

542 Ragheb S (2018) Removal of Heavy Metals from Wastewater Using Sewage Sludge Ash (SSA) as  
543 Adsorbent. SSRN Electron J. <https://doi.org/10.2139/ssrn.3164094>

544 Rashed MN (2018) Heavy Metals Removal from Wastewater by Adsorption on Modified Physically  
545 Activated Sewage Sludge. Arch Org Inorg Chem Sci 1:.  
546 <https://doi.org/10.32474/aoics.2018.01.000102>

547 Ryssel ST, Arvin E, Lützhøft HCH, et al (2015) Degradation of specific aromatic compounds migrating  
548 from PEX pipes into drinking water. Water Res 81:269–278.  
549 <https://doi.org/10.1016/j.watres.2015.05.054>

550 Setia R, Rengasamy P, Marschner P (2014) Effect of mono- and divalent cations on sorption of water-  
551 extractable organic carbon and microbial activity. Biol Fertil Soils 50:727–734.  
552 <https://doi.org/10.1007/s00374-013-0888-1>

553 Shahat AA, Ibrahim AY, Hendawy SF, et al (2011) Chemical composition, antimicrobial and antioxidant  
554 activities of essential oils from organically cultivated fennel cultivars. Molecules 16:1366–1377.  
555 <https://doi.org/10.3390/molecules16021366>

556 Singh DK, Mondal S, Chakravartty JK (2016) Recovery of Uranium from Phosphoric Acid: A Review.  
557 Solvent Extr Ion Exch 34:201–225. <https://doi.org/10.1080/07366299.2016.1169142>

558 Stewart WM, Roberts TL (2012) Food security and the role of fertilizer in supporting it. In: Procedia  
559 Engineering. pp 76–82

560 Taha MH, Abdel Maksoud SA, Ali MM, et al (2019) Conversion of biomass residual to acid-modified  
561 bio-chars for efficient adsorption of organic pollutants from industrial phosphoric acid: an  
562 experimental, kinetic and thermodynamic study. Int J Environ Anal Chem 99:1211–1234.  
563 <https://doi.org/10.1080/03067319.2019.1618459>

564 Taha MH, El-Maadawy MM, Hussein AEM, Youssef WM (2018) Uranium sorption from commercial  
565 phosphoric acid using kaolinite and metakaolinite. J Radioanal Nucl Chem 317:685–699.

566 <https://doi.org/10.1007/s10967-018-5951-9>

567 US National Library of Medicine (2020) Butylated hydroxytoluene | C15H24O - PubChem

568 Wheeler DL, Chappey C, Lash AE, et al (2000) Database resources of the National Center for  
569 Biotechnology Information. *Nucleic Acids Res.* 28:10–14

570 Wołowiec M, Bajda T (2017) Current stage of knowledge relating to the use ferruginous sludge from  
571 water treatment plants-a preliminary review of the literature. *MINERALOGIA* 48:39–45.  
572 <https://doi.org/10.1515/mipo-2017-0010>

573 Wołowiec M, Komorowska-Kaufman M, Pruss A, et al (2019) Removal of heavy metals and metalloids  
574 from water using drinking water treatment residuals as adsorbents: A review. *Minerals* 9

575 Wu FC, Tseng RL, Juang RS (2009) Initial behavior of intraparticle diffusion model used in the  
576 description of adsorption kinetics. *Chem Eng J* 153:1–8. <https://doi.org/10.1016/j.cej.2009.04.042>

577 Yu L, Zhong Q (2006) Preparation of adsorbents made from sewage sludges for adsorption of organic  
578 materials from wastewater. *J Hazard Mater* 137:359–366.  
579 <https://doi.org/10.1016/j.jhazmat.2006.02.007>

580 Zhang M, Zhang H (2010) Co-transport of dissolved organic matter and heavy metals in soils induced  
581 by excessive phosphorus applications. *J Environ Sci* 22:598–606. [https://doi.org/10.1016/S1001-  
582 0742\(09\)60151-0](https://doi.org/10.1016/S1001-0742(09)60151-0)

583 Zhang R, Chen C, Li J, Wang X (2015) Preparation of montmorillonite@carbon composite and its  
584 application for U(VI) removal from aqueous solution. *Appl Surf Sci* 349:129–137.  
585 <https://doi.org/10.1016/j.apsusc.2015.04.222>

586 Zou Y, Wang X, Wu F, et al (2017) Controllable Synthesis of Ca-Mg-Al Layered Double Hydroxides  
587 and Calcined Layered Double Oxides for the Efficient Removal of U(VI) from Wastewater  
588 Solutions. *ACS Sustain Chem Eng* 5:1173–1185. <https://doi.org/10.1021/acssuschemeng.6b02550>

589 (2020) National Center for Biotechnology Information, PubChem Compound Summary for CID 3026,

590 Dibutyl phthalate. In: Natl. Cent. Biotechnol. Inf.  
591 <https://pubchem.ncbi.nlm.nih.gov/compound/Potassium-ion>.

592

# Figures

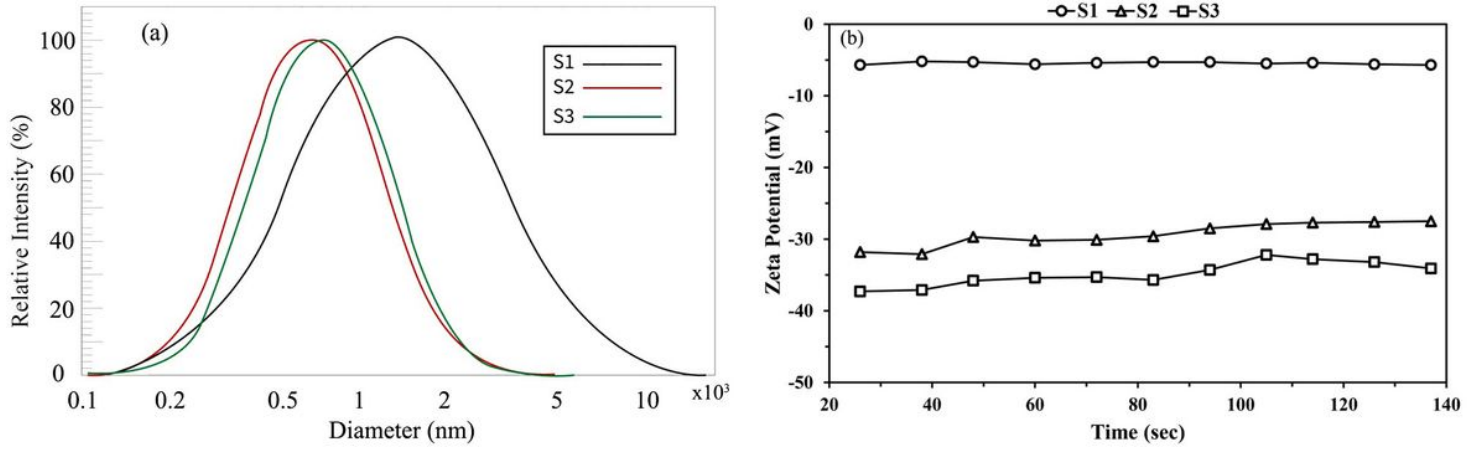


Figure 1

a: Particle size distribution of WTS samples. b: Zeta potential of different WTS samples.

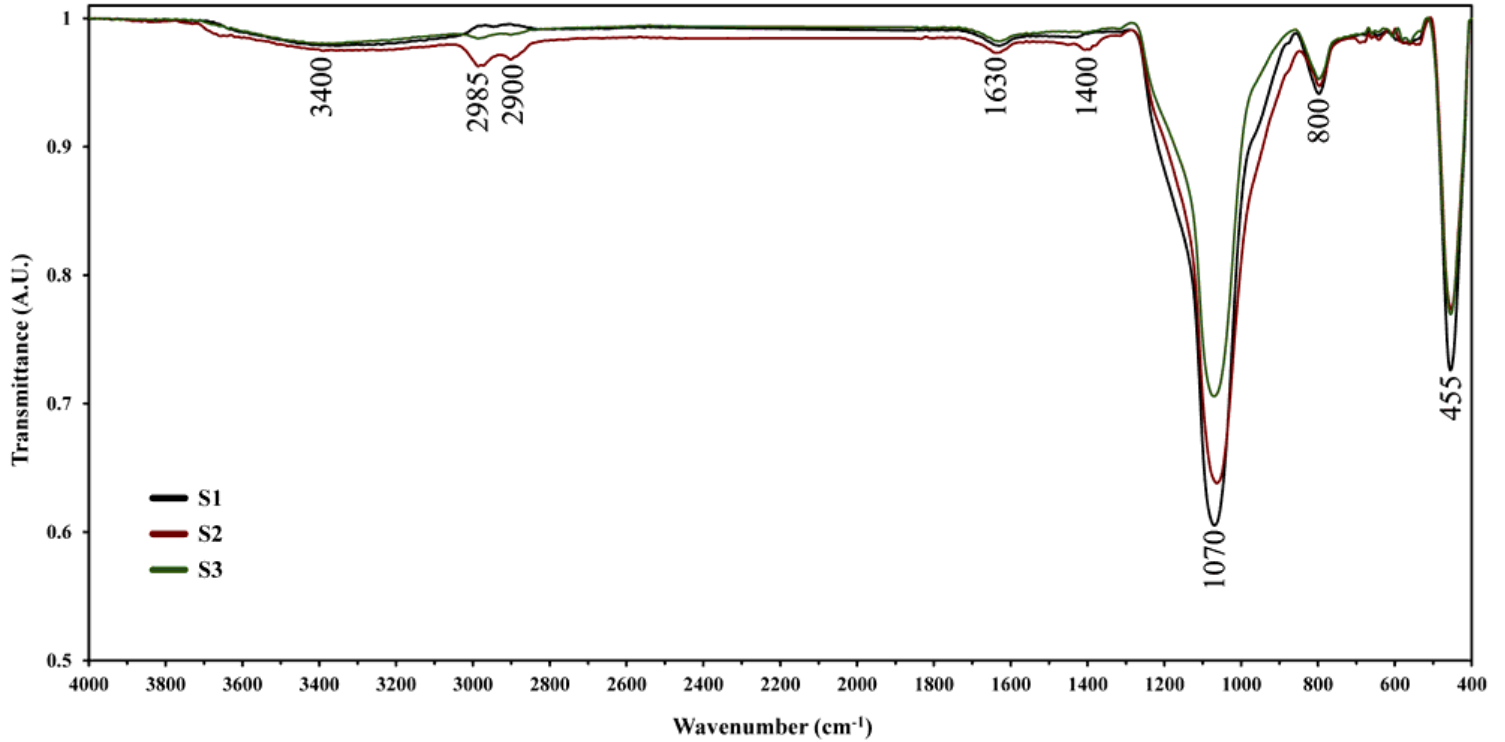
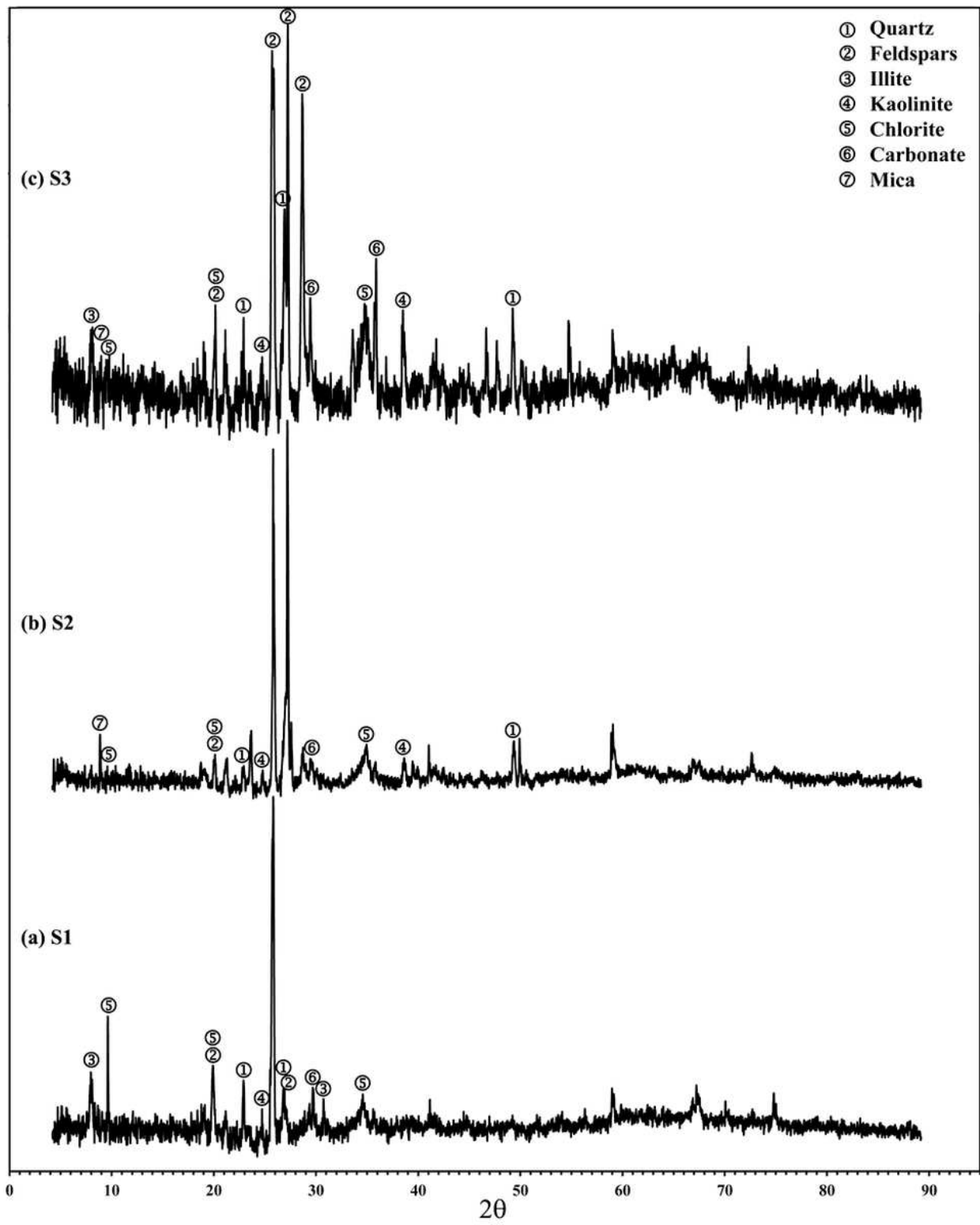


Figure 2

FTIR spectra of WTS samples.



**Figure 3**

X-ray diffraction patterns of WTS samples.

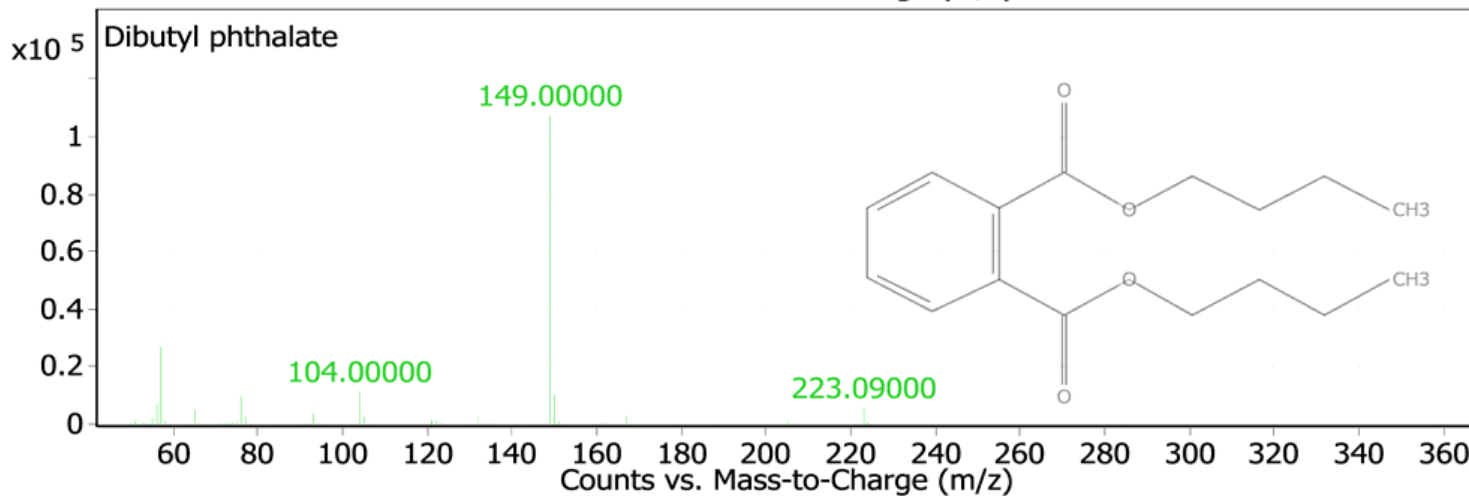
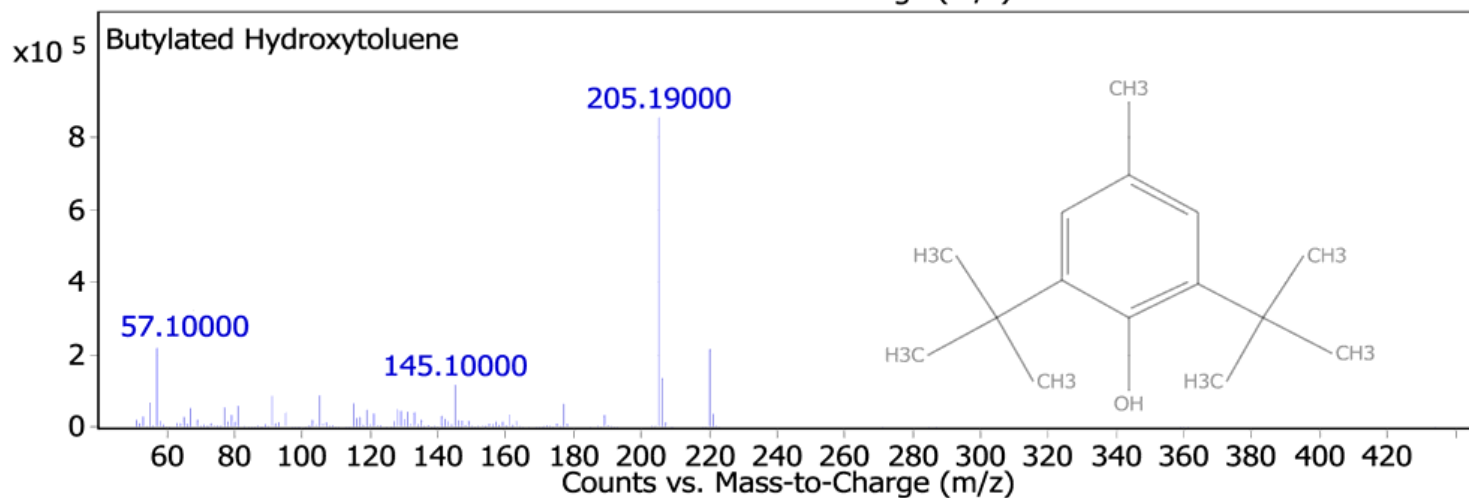
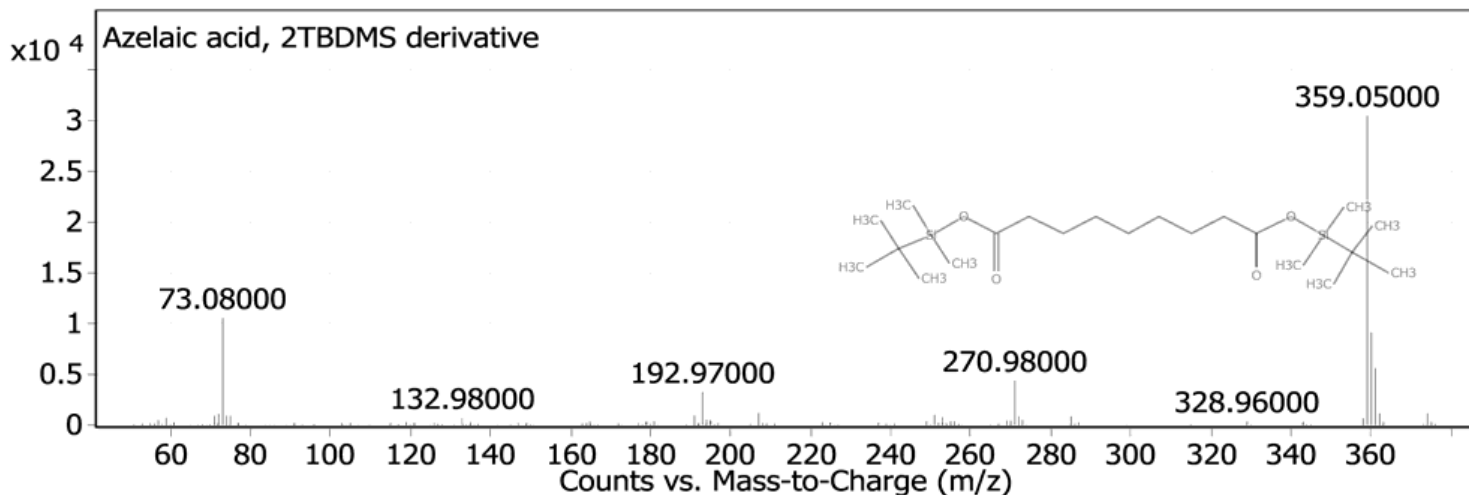


**Figure 4**

The main organic components in the crude phosphoric acid

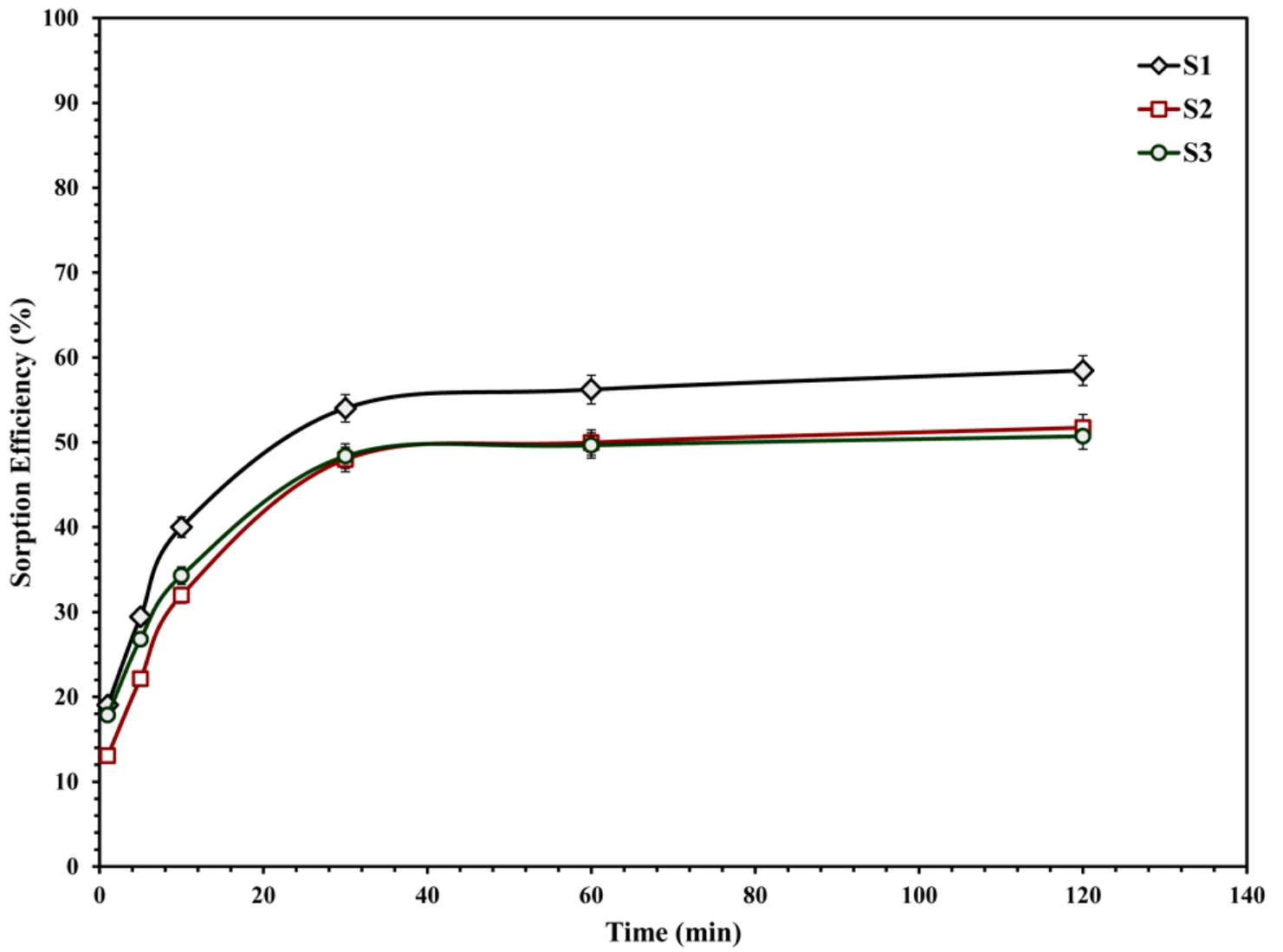


Figure 5

Organic matter sorption efficiency as a function of shaking time.

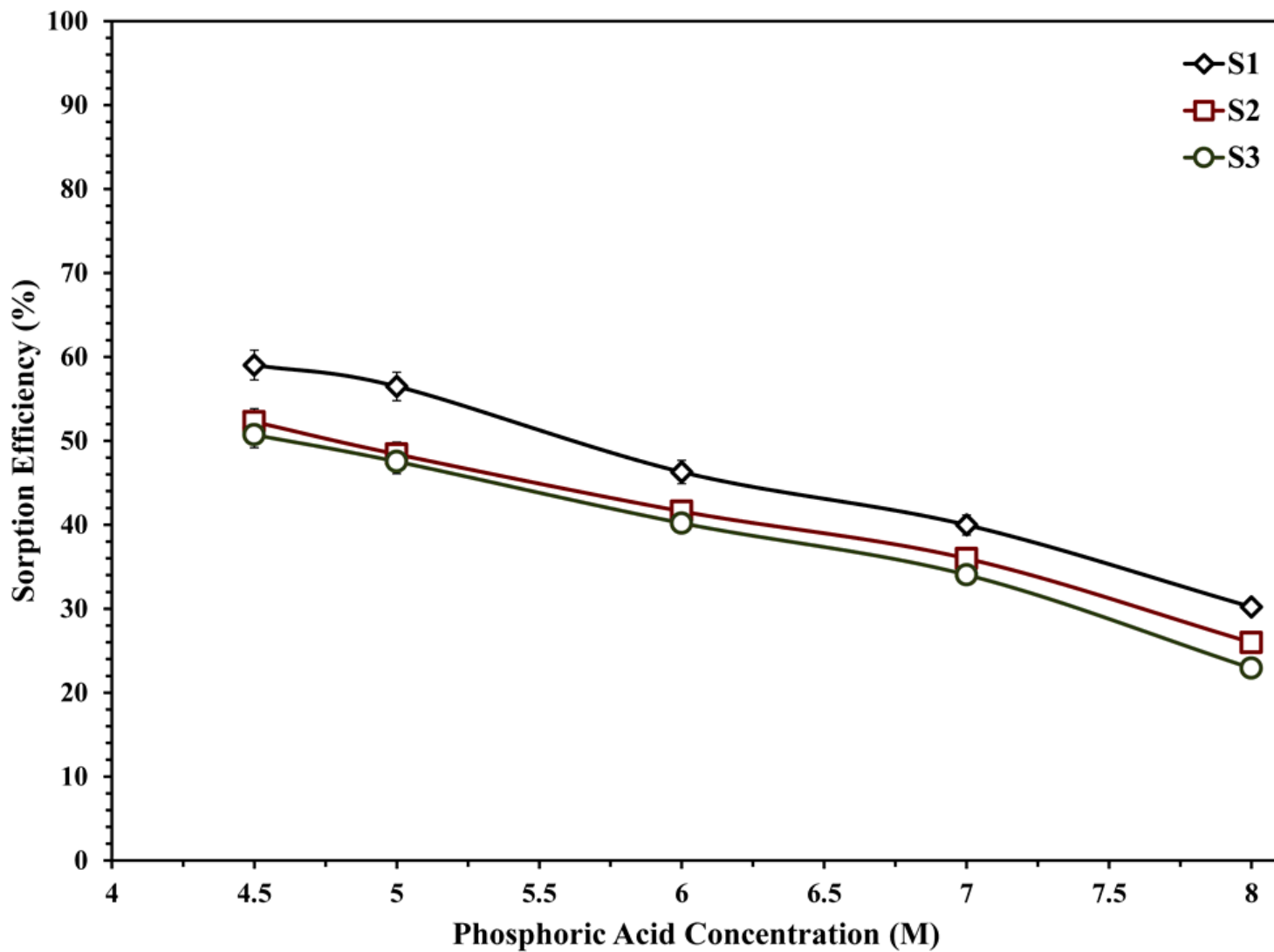


Figure 6

Organic matter sorption efficiency as a function of phosphoric acid concentration.

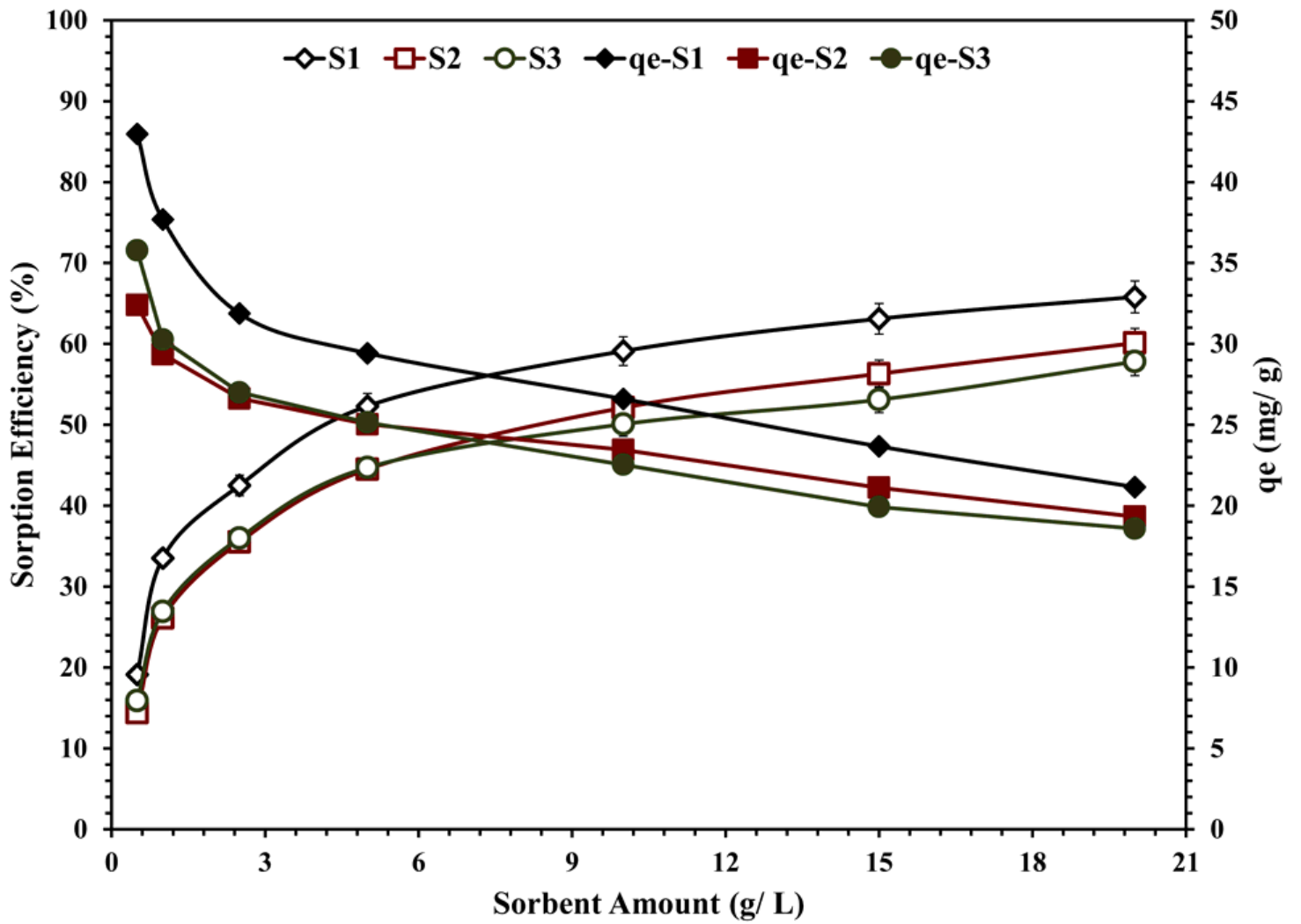


Figure 7

Organic matter sorption efficiency as a function of sorbent amount of addition.

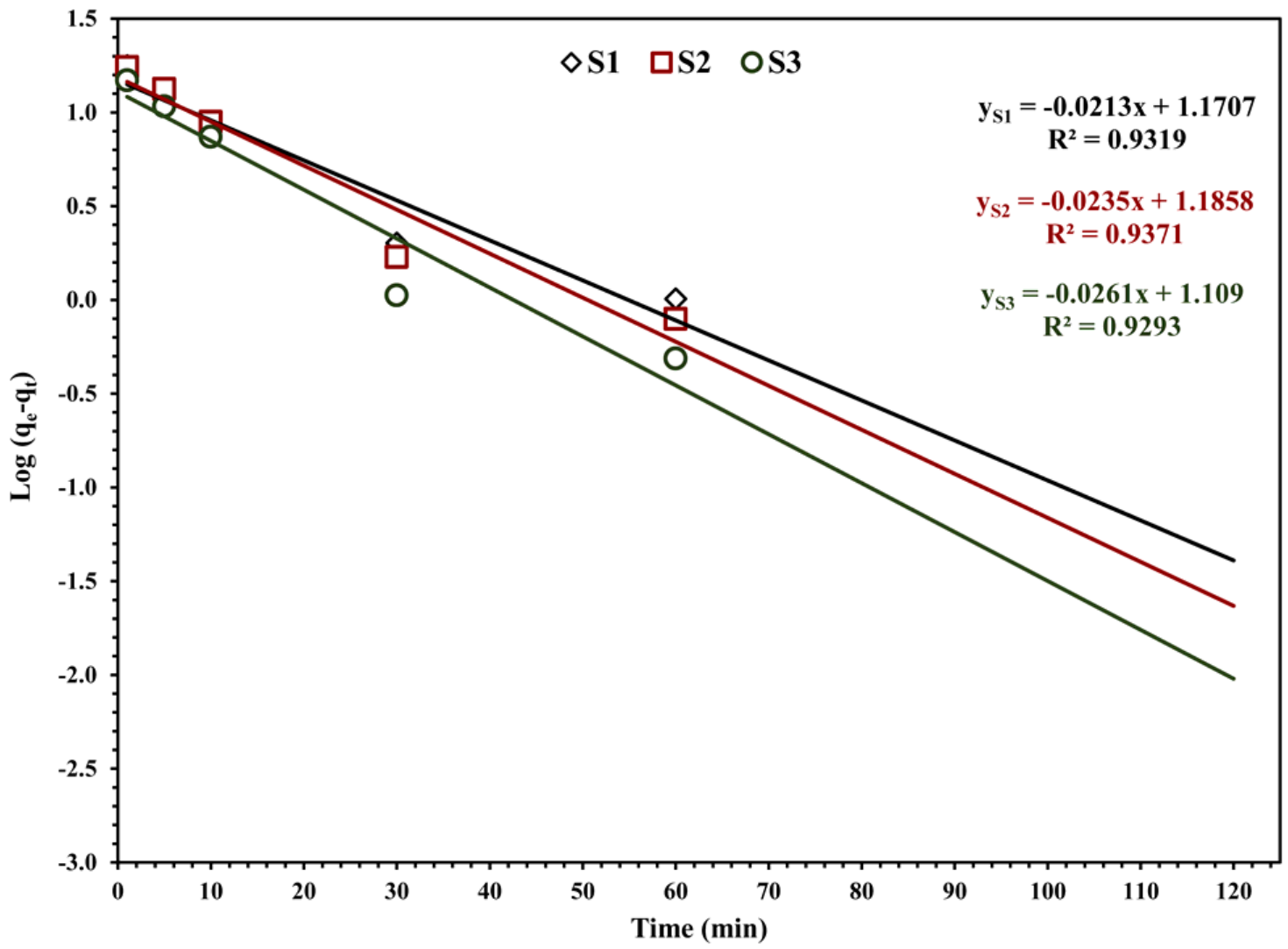


Figure 8

Lagergreen plot for organic matter sorption using WTS.

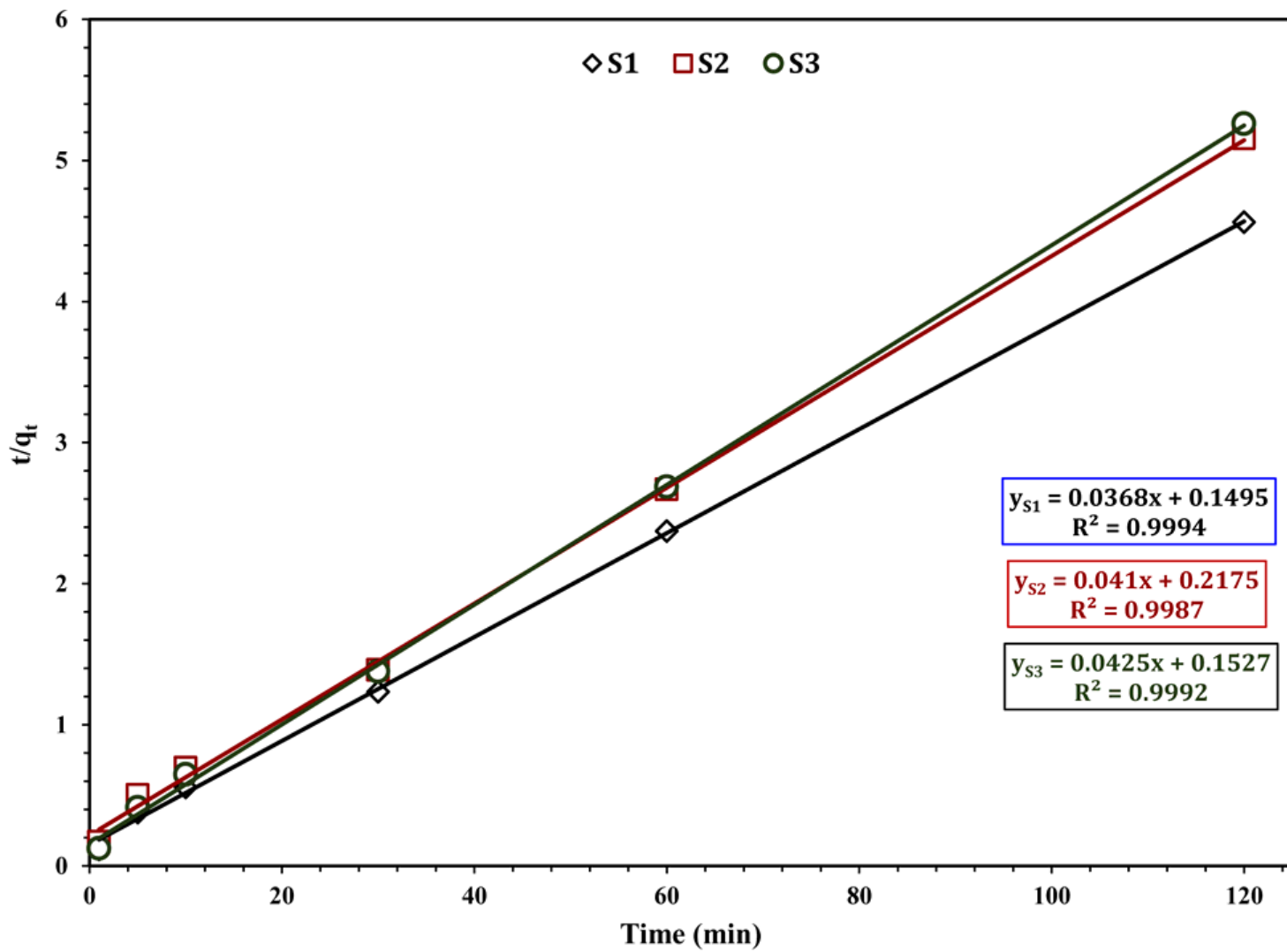


Figure 9

Pseudo second-order plot for organic matter sorption using WTS.

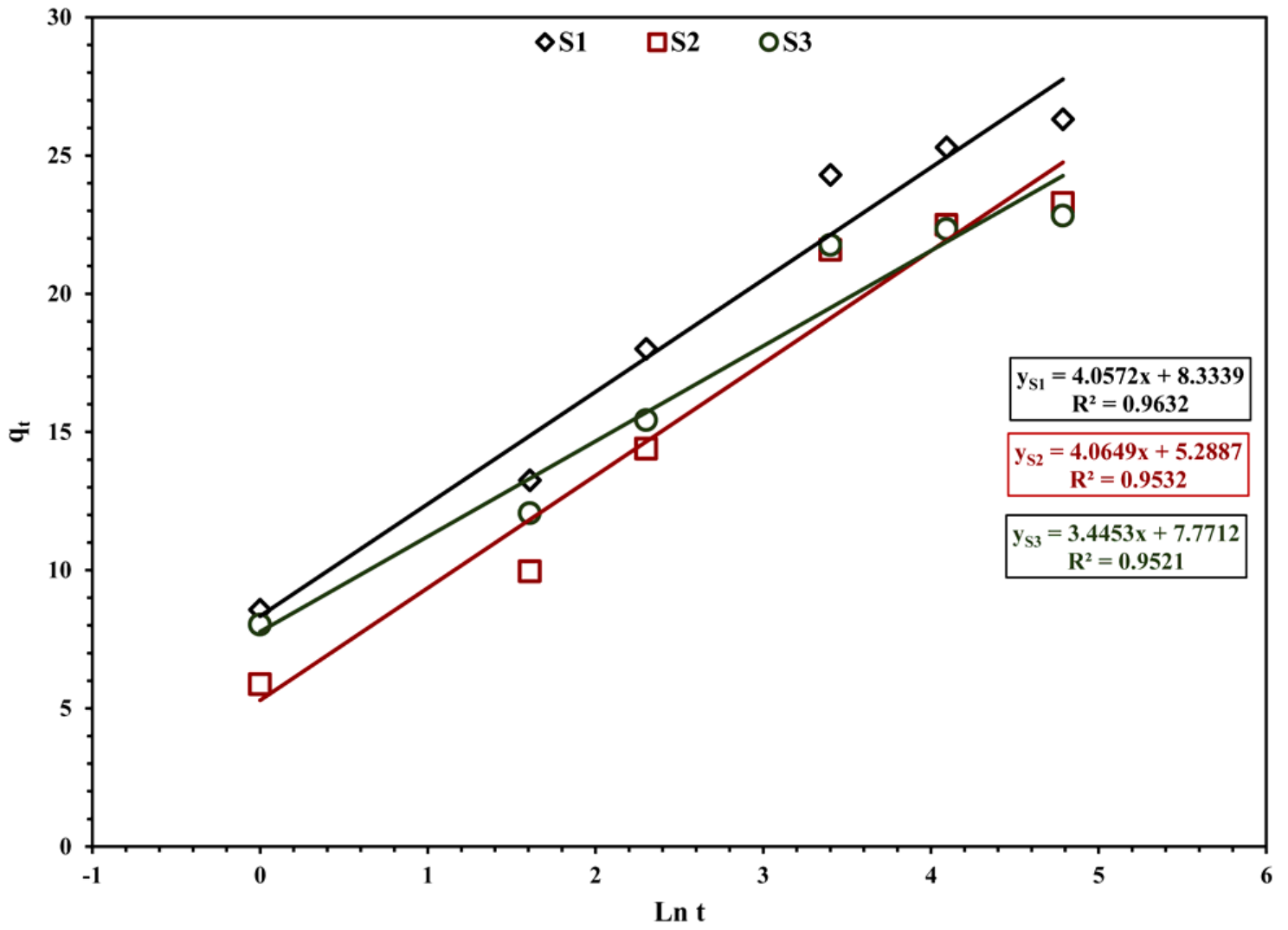


Figure 10

Elovich model plot for organic matter sorption using WTS.

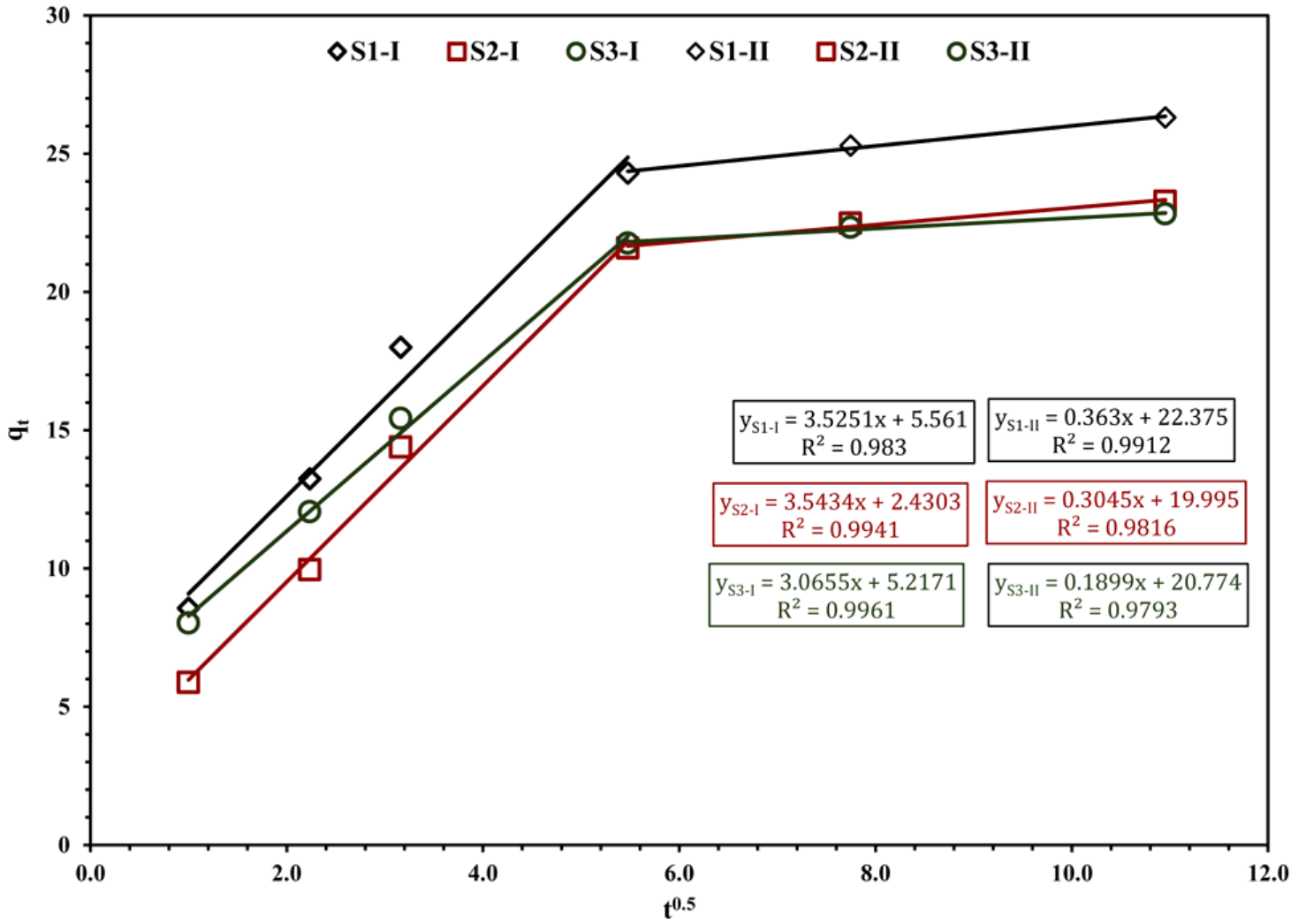


Figure 11

Weber and Morris illustration for organic matter sorption using WTS.

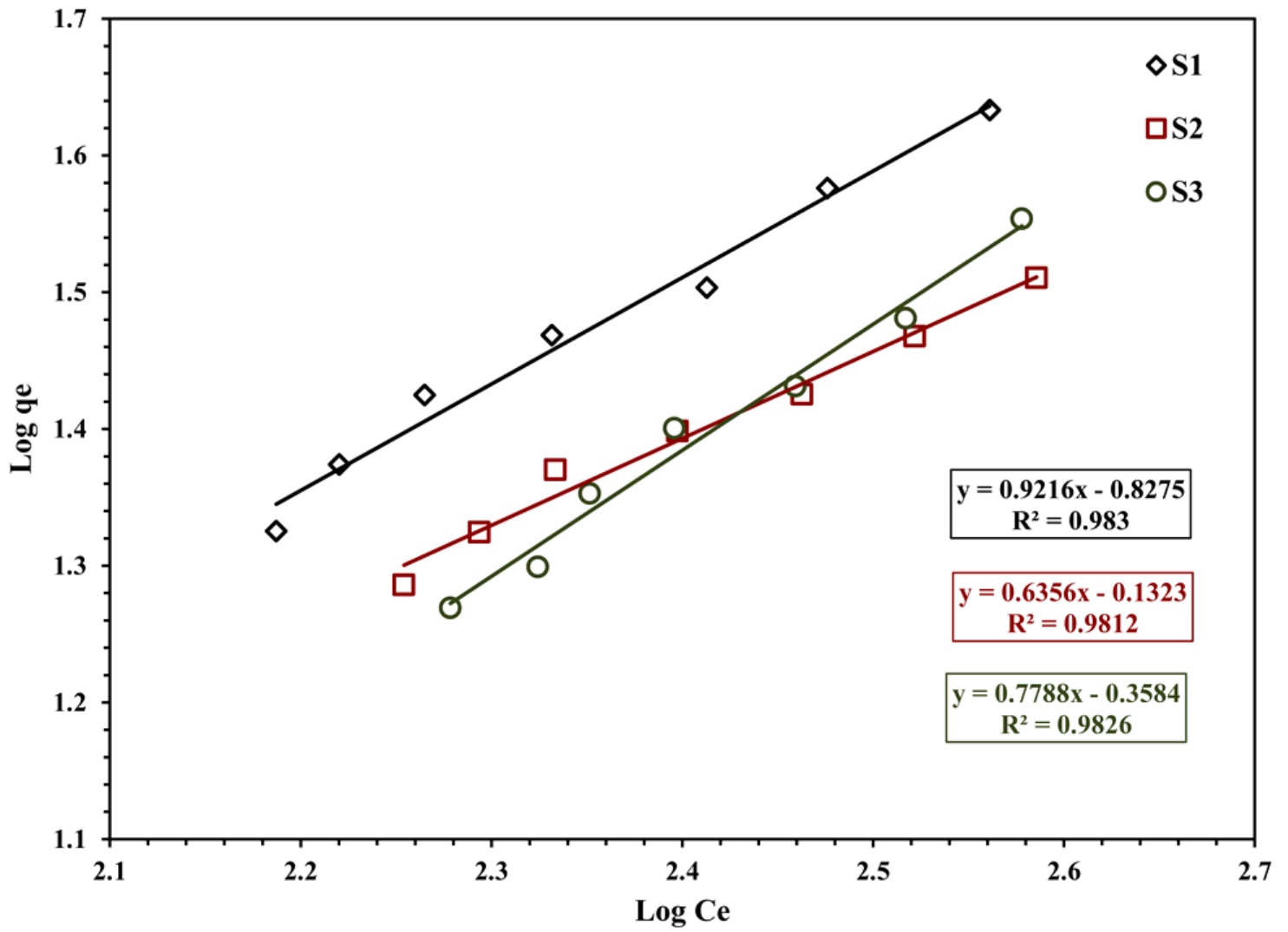


Figure 12

Freundlich model plot for organic matter sorption using different WTS samples.

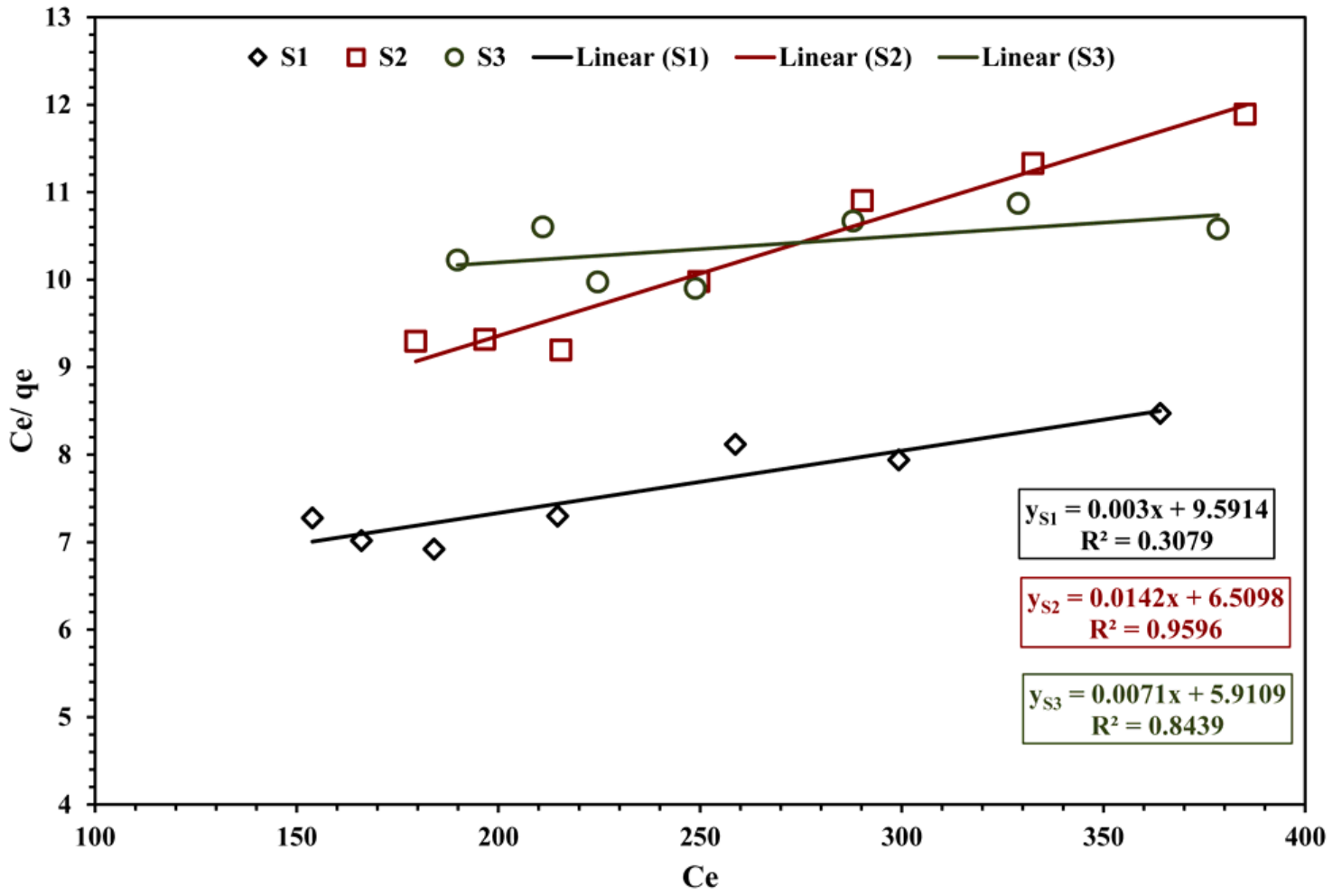


Figure 13

Langmuir model plot for organic matter sorption using different WTS samples.